Machine Learning-Based Spatial Modeling of Land Surface Temperature in Butantã: Insights from SHAP Interpretability

Williane G. S. Pereira[1,2], Gabriel V. de Melo[2], Waldemiro J. A. G. Negreiros[1], Fernando A. R. Costa[1], Leonardo de O. Tamasauskas[1,2], Claudomiro de S. de S. Junior[2], Marcos C. R. Seruffo[1]

[1]Laboratório de Pesquisa Operacional (LPO)
Laboratory of Intelligent Interactive Systems (LIIS)
Universidade Federal do Pará (UFPA), Belém-PA

[2]Faculdade de Computação (FACOMP)
Instituto de Ciências Exatas e Naturais (ICEN)
Universidade Federal do Pará (UFPA), Belém-PA

williane.pereira@icen.ufpa.br, gabriel.melo@icen.ufpa.br,
leonardo.tamasauskas@icen.ufpa.br, waldemiro.negreiros@ifpa.edu.br,
fernando.augusto.mlr@gmail.com, cssj@ufpa.br, seruffo@ufpa.br

Abstract. *Accelerated urbanization has expanded urban heat islands, necessitating the precise monitoring of Land Surface Temperature (LST). This study spatially predicts LST in Butantã (SP) for 2018 and 2021 using a high-resolution multiscale approach. To capture the relationships between urban morphology and LST, XGBoost and LightGBM models were compared, with XGBoost demonstrating superior predictive performance (R^2 of 0.890 and 0.848). Applying the SHapley Additive exPlanations (SHAP) method to the winning model ensured explainability, revealing the dominance of impervious surfaces in warming, the strong mitigating potential of water bodies and vegetation, and the heat retention induced by topography in valleys.*

1. Introduction

The global trend toward accelerated urban expansion has driven a reconfiguration of natural landscapes, suppressing fundamental ecosystem services in favor of the expansion of gray infrastructure [Ma and Peng 2022]. The massive replacement of vegetation cover with impervious surfaces drastically alters the surface energy balance, reducing evapotranspiration and favoring heat storage [Yin and Zhao 2024]. Consequently, this energy retention results in a systematic increase in Land Surface Temperature (LST), a crucial biophysical parameter for monitoring heat islands.

LST detection is enabled by remote sensing, using thermal sensors on satellites such as Landsat. Despite its relevance, there is a clear gap in research on the capture of thermal heterogeneity at local scales. The use of moderate or coarse resolution orbital data limits the identification of fine-scale dynamics and microclimatic patterns within complex urban environments [Shui et al. 2025]. Consequently, coarse-scale observations are insufficient to accurately characterize how urban morphology modulates heat distribution [Yin and Zhao 2024].

To address these spatial complexities, machine learning algorithms have established themselves as a robust approach in urban climatology [Tamasauskas et al. 2025].

Unlike traditional statistical approaches, these models possess the technical capacity to handle a large volume of variables and the complex nonlinearities that dictate the relationship between urban morphology and LST [Snaiki and Merabtine 2025]. Specifically in the scope of spatial LST prediction, models based on gradient-driven decision trees, such as Extreme Gradient Boosting (XGBoost) and Light Gradient Boosting Machine (LightGBM), have demonstrated superior predictive performance in recent literature [Tanoori et al. 2024, Hoang et al. 2025a, Hoang et al. 2025b].

However, the black box nature of these algorithms poses significant challenges to the explainability of results. This has led to a growing need for the integration of Explainable Artificial Intelligence (XAI) tools, such as the SHapley Additive exPlanations (SHAP) technique [Li et al. 2025]. The application of SHAP ensures interpretability by quantifying the marginal impact of characteristics such as vegetation and imperviousness on LST prediction [Hoang et al. 2025b]. By revealing how specific factors induce thermal variations, SHAP provides urban planners with tools for developing focused mitigation strategies [Arunab and Mathew 2024].

Given this scenario, the objective of this study is to predict and analyze the spatial dynamics of LST in the Butantã district, state of São Paulo (SP), Southeast Brazil, for 2018 and 2021. To address the limitations of the literature, a multiscale approach based on high-resolution data is proposed. The study compares the predictive performance of the XGBoost and LightGBM models to identify the most effective tool for capturing local thermal heterogeneity. Next, the SHAP technique is applied to the best-performing model, enabling interpretation of the influence of urban variables on LST prediction. The aim is to offer practical contributions aligned with Sustainable Development Goal 11 (SDG) and to develop a replicable methodology that supports the planning of resilient, environmentally balanced cities.

2. Materials and Methods

The methodology of this study comprises eight integrated stages, as illustrated in the workflow in Figure 1. These stages range from data acquisition to model interpretability and are detailed in the subsequent subsections.

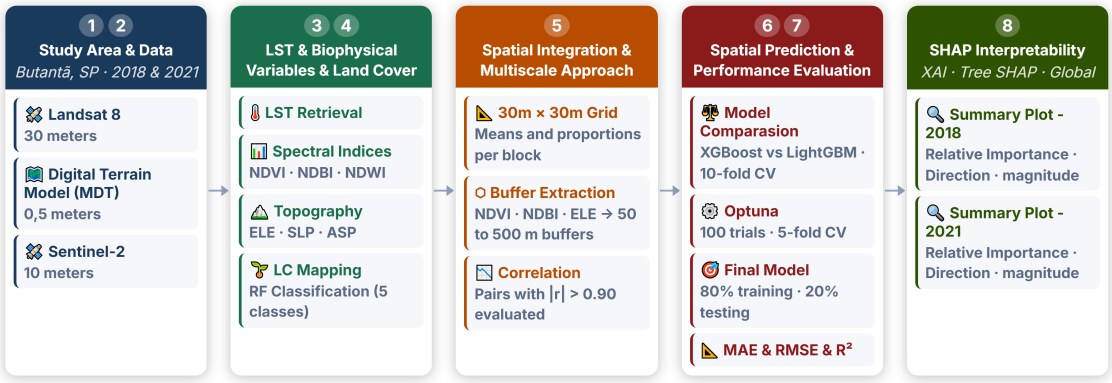

Figure 1. Overview of the research methodological stages.

2.1. Study Area

The study was conducted in the district of Butantã ($23°34'S, 46°43'W$), an administrative unit that is part of the Subprefecture of Butantã [1], in the western zone of the municipality of SP. The study area covers a polygon of approximately $12.5, km^2$ [1], with a regional climate classified as Cwa (humid subtropical), featuring dry winters and mild temperatures [2]. Urbanistically, the region has a morphological duality: on the one hand, it is home to significant areas of urban vegetation (the University of São Paulo (USP) campus and the Butantan Institute) that play a fundamental role in microclimatic regulation [Bueno and Ximenes 2011]; on the other, it includes areas of high building density and intense traffic axes, such as the Raposa Tavares Highway and Vital Brasil Avenue. This scenario configures Butantã as a diverse thermal mosaic, ideal for LST analysis.

2.2. Data Acquisition and Preprocessing

For satellite image acquisition, priority was given to winter in SP (June to August) due to lower cloud cover and reduced atmospheric noise. The years 2018 and 2021 were strategically selected: the former due to its proximity to the 2017 Digital Terrain Model (DTM) used in the study[3], and the lack of consolidated Sentinel-2 imagery in the orbital catalog for the 2017 winter season. The latter was chosen to establish a three-year interval relative to the baseline (2018), to capture changes in land cover and urban morphology. Furthermore, selecting 2021 ensures temporal proximity to the 2020 Digital Surface Model (DSM)[3], enabling the integration of verticalization data in future research stages.

The Sentinel-2 images were obtained from the Harmonized Sentinel-2 MSI (Level-2A) collection of the Copernicus program, with a spatial resolution of 10 meters, acquired on July 16, 2018, and June 5, 2021. The Landsat 8 data, in turn, were extracted from Collection 2 (Level 2, Tier 2), provided by the United States Geological Survey, with a resolution of 30 meters, acquired on August 14, 2018, and June 3, 2021. Both sets were processed in Google Earth Engine (GEE), including cloud masking (QA60 and QA_PIXEL) and application of official scale factors.

In addition to these data, the 2017 DTM was used, available in raster format with a spatial resolution of 0.50 m on the Kaggle platform[3], obtained from the processing of point clouds obtained by Light Detection and Ranging (LiDAR) through the Geosampa portal, from the City of SP. Finally, all layers were clipped using a shapefile from the Brazilian Institute of Geography and Statistics (IBGE, in Portuguese)[4] and reprojected to SIRGAS 2000 / UTM 23S (EPSG: 31983), ensuring spatial consistency between the data.

2.3. LST estimate

The LST was calculated from Band 10 (ST_B10) of the TIRS sensor, processed on the GEE platform. Initially, the digital values were converted to Brightness Temperature (BT) in Kelvin using the official product scale factors (0.00341802 and 149.0). Subsequently, the Land Surface Emissivity (LSE) correction was applied via the Normalized Difference Vegetation Index (NDVI) Threshold Method [Sobrino et al. 2004]. This

[1] https://pt.wikipedia.org/wiki/Butant%C3%A3

[2] https://pt.weatherspark.com/y/30268/Clima-caracter%C3%ADstico-em-S%C3%A3o-Paulo-Brasil-durante-o-ano#google_vignette

[3] https://geosampa.prefeitura.sp.gov.br/PaginasPublicas/_SBC.aspx

[4] https://www.geoaplicada.com/dados/distritos-e-subdistritos/

method uses the Vegetation Proportion (P_v) derived from NDVI to parameterize each pixel's emissivity. Finally, the LST was obtained by inverting Planck's Law corrected for emissivity [Kim et al. 2022] (Equation 1).

$$LST(^{\circ}C) = \frac{BT}{1 + \left(\frac{0{,}00115 \cdot BT}{1{,}4388}\right) \cdot \ln(LSE)} - 273,15 \quad (1)$$

2.4. Biophysical and Land Cover Variables

From Sentinel-2 images, spectral indices were derived that are decisive in modeling LST heterogeneity [Hoang et al. 2025a, Arunab and Mathew 2024]. NDVI functions as a mitigating factor by promoting biomass cooling; the Normalized Difference Built-up Index (NDBI) serves as a thermal inducer via impervious surfaces; and the Normalized Difference Water Index (NDWI) contributes to thermal stabilization [Ma and Peng 2022]. The formulation of these indices followed standard equations consolidated in the literature [Kim et al. 2022]. Additionally, topographic variables were derived from the DTM, including elevation (in meters), slope (in degrees), and aspect (in degrees), with the latter defining surface orientation relative to solar insolation. Although their isolated effects are often limited, their interaction with biophysical indicators plays an important role in explaining LST heterogeneity [Raufu and Adediran 2025].

Acquisition of ground-cover data from Sentinel-2 images yielded five classes: ground vegetation, wooded areas, urbanized areas, water bodies, and exposed soil. The training set consisted of 100 randomly selected points per class for each year (2018 and 2021), supplemented with samples from 2024 to strengthen the overall dataset. The Random Forest (RF) algorithm implemented in the GEE plataform was chosen, justified by its consolidated performance in land cover mapping [Hoang et al. 2025a]. The model used 70% of the data for training, integrating bands B2 to B12 and the collected indices.The script is available in the GitHub repository [5].

Finally, performance was evaluated using the Kappa metric, a coefficient that measures the model's actual agreement by penalizing random hits, as described in Landis and Koch (1977). The evaluation yielded a Kappa of 92%, classifying it as "almost perfect" agreement according to the authors' criteria.

2.5. Spatial Integration and Multiscale Approach

To align the data, a 30 m × 30 m grid was generated to match the spatial resolution of the LST pixels, resulting in 14,065 urban blocks per year. For each block, LST values, topographic means, and spectral indices were extracted, along with land cover proportions, enabling the synthesis of local microclimatic morphology and the evaluation of urban influence on temperature. Furthermore, to analyze how environmental factors external to the block influence internal heat, a multiscale extraction of NDVI, NDBI, and elevation was conducted within radii ranging from 50 to 500 meters, centered on each block. This multiscale framework follows Kim et al. (2022), who demonstrated that neighborhood-scale variables are highly decisive in predicting local LST.

[5] `https://github.com/Williane28/Urban-land-classification-WCAMA`

Additionally, the elevation difference between the observed block and its respective radii was used to calculate the Topographic Position Index (TPI), which indicates whether the block lies in higher or lower areas, whose influence is analyzed in Hoang et al. (2022b). After processing, 41 explanatory variables were obtained per year. To reduce dimensionality and redundancy, a correlation analysis was performed between the independent variables and between them and the LST; whenever a pair exhibited an absolute correlation greater than 90%, the variable with the lower correlation with the LST was removed, yielding 19 consolidated predictive variables.

For textual and graphical standardization, the following nomenclature was adopted: average metrics for the block as NDVI_MEAN, NDBI_MEAN, NDWI_MEAN, ELE_MEAN (elevation), SLP_MEAN (slope), and ASP_MEAN (aspect); land cover proportions such as WAT_PROP (water bodies), BARE_PROP (bare land), TREE_PROP (tree vegetation), HERB_PROP (herbaceous vegetation), and URB_PROP (urbanized area); and multiscale variables with distance suffix, for instance, TPI_mean_Xm, NDVI_mean_Xm, NDBI_mean_Xm, where X represents the radius in meters.

2.6. Spatial Predictive Modeling of LST and Evaluation

The spatial prediction of LST was conducted independently for each analyzed year, using a comparative evaluation of two Gradient-Boosted Decision Tree (GBDT) algorithms: XGBoost and LightGBM. Both models are composed of a sequential combination of multiple weak learners, whose final predictions are obtained as a weighted sum of small regressions, thereby capturing complex and nonlinear patterns [Snaiki and Merabtine 2025]. The choice of these architectures was based on their proven convergence and robustness in similar studies of urban thermal dynamics [Li et al. 2025, Tanoori et al. 2024]. Predictive performance was validated using the 10-fold cross-validation technique, aiming to identify the most accurate model for capturing local thermal dynamics and ensuring the generalization of the results.

The Optuna framework was used to optimize the hyperparameters of the best-performing model. Unlike exhaustive grid search or random search methods, Optuna uses Bayesian optimization, specifically the Tree-structured Parzen Estimator (TPE) algorithm, to intelligently explore the hyperparameter space [Akiba et al. 2019]. In the present study, an automatic search was conducted over 100 iterations (trials) to maximize the objective function based on the Coefficient of Determination (R^2) obtained from 5-fold cross-validation. Finally, to consolidate the final models for each scenario, the data were partitioned into a training set (80%) and a test set (20%), applying the optimal optimization settings.

To evaluate the models in the comparative analysis and validate the predictive performance of the final model, the metrics Mean Absolute Error (MAE), Root Mean Square Error (RMSE), and R^2 were adopted, consistent with their application in research on LST [Hoang et al. 2025b, Arunab and Mathew 2024]. Each metric provides a complementary perspective on the model's performance: both MAE and RMSE allow a direct physical interpretation of the magnitude of the error in the same unit as the target variable ($^{\circ}C$), with MAE being less sensitive to extreme values and RMSE being more rigorous with large deviations; and R^2 indicates the proportion of LST variability that is effectively explained by the urban and environmental attributes used.

2.7. Interpretability via SHAP

As a final step, the SHAP technique was integrated into the final model to mitigate the black box nature of machine learning models. SHAP is an XAI method based on Cooperative Game Theory that quantifies the marginal contribution of each explanatory variable to the model's final result [Lundberg et al. 2018].

The framework computes Shapley Values, which represent a mathematically consistent distribution of each feature's marginal contribution to the final prediction. SHAP is based on the property of local accuracy, which ensures that the sum of the contributions of each explanatory variable exactly recovers the difference between the individual prediction of a sample and the overall mean of the model. In this study, the Tree SHAP algorithm was used, as it is optimized for tree-ensemble architectures and ensures high computational efficiency and global consistency [Lundberg et al. 2018]. The application of this technique allows for two levels of analysis: (i) global, identifying the most influential predictors in the overall behavior of the prediction; and (ii) local, explaining the specific influences of each variable on individual samples.

3. Results

3.1. Model Comparison and LST Prediction

In this step, the predictive performance of the XGBoost and LightGBM algorithms was evaluated and compared for the years 2018 and 2021. Table 1 presents the performance metrics obtained after cross-validation. These results highlight each model's ability to capture the spatial variability of LST in Butantã.

In all scenarios analyzed, the XGBoost model outperformed LightGBM. According to Table 1, XGBoost obtained higher R^2 values, indicating a greater ability to explain LST variance based on the set of independent variables adopted. Furthermore, the reduction in error metrics (MAE and RMSE) suggests that the algorithm is less prone to large-magnitude errors, thereby improving prediction stability and accuracy. In summary, the model has established itself as the most robust tool for modeling local thermal dynamics in the study area.

Table 1. Performance of XGBoost and LightGBM models for 2018 and 2021.

	XGBoost		**LightGBM**	
Metric	**2018**	**2021**	**2018**	**2021**
R^2	**0,8682**	**0,8193**	0,8538	0,7936
MAE (°C)	**0,4719**	**0,4414**	0,5084	0,4811
RMSE (°C)	**0,6212**	**0,5810**	0,6542	0,6211

With XGBoost established as the most suitable model, the subsequent stage of the study focused on its technical refinement. To maximize its potential, a rigorous hyperparameter optimization of nine key variables was conducted, following Kim et al. (2022) . The complete optimization results are available in the source code on GitHub[6].

[6]https://github.com/Williane28/Urban-LST-XAI-WCAMA

Following this stage, the final models were trained using the optimal hyperparameter settings for each year. The resulting predictions demonstrated high accuracy, as evidenced by R^2 values of 0.890 (2018) and 0.848 (2021), indicating a robust capacity to explain the spatial variance of LST. The precision of these estimates is further supported by the low residual errors, yielding MAE metrics of 0.421 °C (2018) and 0.398 °C (2021), and RMSE values of 0.570 °C and 0.526 °C, respectively.

3.2. SHAP analysis

Figure 2 shows the Summary Plot, which summarizes three crucial pieces of information for each explanatory variable: (i) relative importance, given by the position on the vertical axis; (ii) the magnitude and direction of the impact on the prediction, indicated by the position on the horizontal axis, where positive SHAP values indicate an increase in LST and negative values indicate a decrease; and (iii) the original value of the variable, represented by the color scale, where red indicates high values and blue indicates low values. Each point on the graph represents an individual urban block within study area.

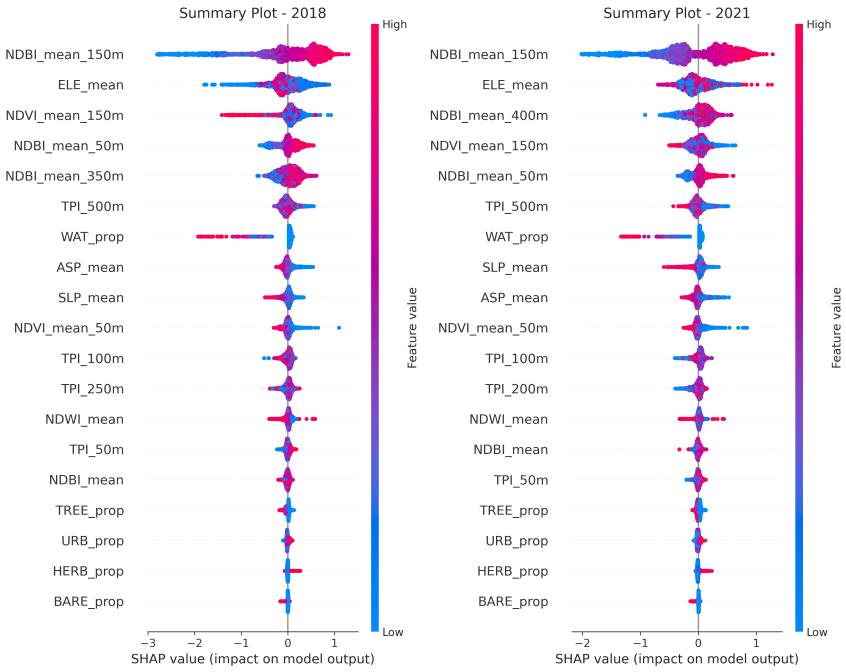

Figure 2. SHAP Analysis: Overall Importance and Direction of Explanatory Variables.

The analysis of the results reveals consistent patterns of influence of the predictor variables in 2018 and 2021. In both periods, the NDBI index, within a radius of 150 meters, emerged as the most influential predictor, with positive contributions reaching approximately 1.0 ºC in SHAP values for certain urban blocks. Elevation (ELE_mean) was the second most relevant factor; though it exhibited nonlinear behavior, low-altitude areas were associated with both positive and negative LST deviations. In the 2018 scenario, high-altitude regions showed a more distinct inverse relationship with LST compared to 2021, characterized by a stronger negative SHAP contribution (shifting predictions below the mean).

Regarding urban influence scales, the hierarchy of importance has reversed between the two years. In 2021, regional imperviousness (NDBI_mean_400m) surpassed the relevance of local vegetation (NDVI_mean_150m), with positive contributions to thermal prediction. Conversely, in 2018, the negative effect of local vegetation (NDVI_mean_150m) surpassed the positive influences of regional (NDBI_mean_350m) and hyper-local (NDBI_mean_50m) scales. The TPI_500m variable maintained a consistent pattern of relevance across both years: high values (peaks) are associated with decreases in predicted LST, whereas low values (valleys) are associated with increases in predicted LST.

Although rare in the samples, the presence of the hydrological variable (WAT_prop) leads to SHAP values exceeding -2.0 °C in both years. Other variables, such as aspect, slope, and NDVI at 50 meters, had a marginal negative impact, while the remaining variables had an impact close to zero, indicating low influence on the final model prediction.

4. Discussion

The high performance of the XGBoost model corroborates the literature [Arunab and Mathew 2024, Tanoori et al. 2024]. While direct numerical comparisons are constrained by variations in datasets and geographical contexts, the R^2 values obtained in this study are consistent with the predictive standards reported in similar modeling frameworks [Hoang et al. 2025a, Kim et al. 2022]. Furthermore, the minimal deviations observed in the MAE and RMSE metrics underscore a strong capacity to capture the spatial heterogeneity of LST. This level of accuracy is particularly significant in high-resolution contexts, where fine-scale detail introduces microclimatic complexities that may present challenges to predictive capacity. Ultimately, these reduced errors confirm the model's fidelity in representing the biophysical relationships that govern LST at the urban block scale.

The SHAP analysis revealed a multiscale "thermal personality" for Butantã, in which the interaction between the built environment and topography shapes LST patterns. The dominance of NDBI_mean_150m in the two years analyzed reaffirms the essential role of impervious surfaces in the deterioration of thermal stress, while the negative influences presented by NDVI and WAT_prop highlight the potential of vegetation and water bodies as mitigating agents [Ma and Peng 2022]. However, this dynamic is sensitive to scale: the observed transition to regional dominance (NDBI_mean_400m) in 2021 suggests that local cooling (NDVI_mean_150m) may be offset by urban pressures from wider surrounding areas. This phenomenon of "thermal overflow" by advection [Shui et al. 2025] indicates that, in scenarios of high thermal connectivity, planning must go beyond the lot scale and consider neighborhood-scale vegetation barriers to block the flow of sensible heat [Bai et al. 2024].

Furthermore, the hierarchy of importance of elevation over aspect and slope aligns with studies using SHAP analysis to reveal the topographic control of LST [Hoang et al. 2025a, Kim et al. 2022]. The TPI behavior by SHAP, which classifies hilltops as cooling zones and valley bottoms as thermal traps, corroborates the findings of Hoang et al. (2025b), who reported a negative correlation between TPI and LST. In urban planning, this suggests that preserving wind corridors and controlling vertical

development on hilltops can be effective for cooling neighborhoods.

Despite the advances, this study has limitations that open avenues for future research. First, satellite-derived LST data may contain atmospheric noise and uncertainties inherent to the LST retrieval process, which would be better validated with in situ thermal measurements. In addition, the analysis was restricted to specific time periods, failing to account for seasonal variability that alters vegetation phenology and the urban energy balance. The absence of verticalization data, such as buildings and Sky View Factor (SVF), also limits a complete understanding of shading and radiation retention.

5. Conclusion

This study proposed a high-resolution multiscale approach to predict and analyze LST dynamics in the Butantã neighborhood of SP in 2018 and 2021 scenarios. By evaluating the XGBoost and LightGBM algorithms, the superiority of XGBoost in capturing complex nonlinear relationships between urban morphology and local thermal patterns was confirmed, with high predictive accuracy (R^2 values of 0.890 and 0.848, respectively). By employing SHAP, this study moved beyond the "black-box" limitations of the XGBoost model, offering a transparent view of the biophysical drivers behind LST variability.

The analysis revealed that impermeabilization (NDBI) within a 150-meter radius is the primary driver of local warming. A dynamic multiscale importance was also found: the cooling provided by vegetation at 150 meters in 2018 was surpassed by the influence of impervious surfaces (NDBI) on a larger scale (400 meters) in 2021. In contrast to this warming effect, water bodies (WAT_prop) and vegetation (NDVI) proved to be strong mitigating agents, whereas valleys act as hot-air zones. These findings aim to inform urban planning, emphasizing the importance of preserving ventilation corridors and adopting nature-based solutions at both the lot and neighborhood scales.

For future work, it is recommended that seasonal data be incorporated to understand phenological responses throughout the year. Additionally, the inclusion of verticalization and SVF data is a fundamental step in simultaneously measuring the impact of building shading and the effect of heat retention on roads. Thus, the aim is to improve the scientific basis necessary for planning more resilient cities (SDG 11).

References

Akiba, T., Sano, S., Yanase, T., Ohta, T., and Koyama, M. (2019). Optuna: A next-generation hyperparameter optimization framework. In *The 25th ACM SIGKDD International Conference on Knowledge Discovery & Data Mining*, pages 2623–2631.

Arunab, K. and Mathew, A. (2024). Exploring spatial machine learning techniques for improving land surface temperature prediction. *Kuwait Journal of Science*, 51(3):100242.

Bai, X., Yu, Z., Wang, B., Zhang, Y., Zhou, S., Sha, X., Li, S., Yao, X., and Geng, X. (2024). Quantifying threshold and scale response of urban air and surface temperature to surrounding landscapes under extreme heat. *Building and Environment*, 247:111029.

Bueno, E. S. and Ximenes, D. S. S. (2011). A importância da infraestrutura verde no desenho ambiental: Estudo da área da cidade universitária e instituto butantã. *Revista LABVERDE*, (3):128–154.

Hoang, N.-D., Pham, P. A. H., Huynh, T. C., Cao, M.-T., and Bui, D.-T. (2025a). Geospatial urban heat mapping with interpretable machine learning and deep learning: A case study in hue city, vietnam. *Earth Science Informatics*, 18(1):64.

Hoang, N.-D., Tran, V.-D., and Huynh, T.-C. (2025b). From data to insights: Modeling urban land surface temperature using geospatial analysis and interpretable machine learning. *Sensors*, 25(4).

Kim, M., Kim, D., and Kim, G. (2022). Examining the relationship between land use/land cover (lulc) and land surface temperature (lst) using explainable artificial intelligence (xai) models: A case study of seoul, south korea. *International Journal of Environmental Research and Public Health*, 19(23).

Landis, J. R. and Koch, G. G. (1977). The measurement of observer agreement for categorical data. *biometrics*, pages 159–174.

Li, S., Wong, M. S., Zhu, R., Shi, G., and Yang, J. (2025). Impacts of land surface temperature and ambient factors on near-surface air temperature estimation: A multisource evaluation using shap analysis. *Sustainable Cities and Society*, 122:106257.

Lundberg, S. M., Erion, G. G., and Lee, S.-I. (2018). Consistent individualized feature attribution for tree ensembles. *arXiv preprint arXiv:1802.03888*.

Ma, X. and Peng, S. (2022). Research on the spatiotemporal coupling relationships between land use/land cover compositions or patterns and the surface urban heat island effect. *Environmental Science and Pollution Research*, 29(26):39723–39742.

Raufu, I. O. and Adediran, A. (2025). Influence of topographic elements on land surface temperature: A case study using remote sensing and gis. *Journal of Geography, Environment and Earth Science International*, 29(12):249–264.

Shui, C., Shan, B., Li, W., Wang, L., and Liu, Y. (2025). Investigating the influence of land cover on land surface temperature. *Advances in Space Research*, 75(3):2614–2631.

Snaiki, R. and Merabtine, A. (2025). Recent advances on machine learning techniques for urban heat island applications: a review and new horizons. *Sustainable Cities and Society*, page 106943.

Sobrino, J. A., Jiménez-Muñoz, J. C., and Paolini, L. (2004). Land surface temperature retrieval from landsat tm 5. *Remote Sensing of environment*, 90(4):434–440.

Tamasauskas, L. d. O., Pereira, W. G., Negreiros, W. J., Guimaraes, P. H. d. V., Dias, J. A., Corrêa, A. B., Costa, G. B., and Seruffo, M. C. d. R. (2025). Comparison of lstm and sarima models for air temperature forecasting in belém, amazônia, pará. In *Workshop de Computação Aplicada à Gestão do Meio Ambiente e Recursos Naturais (WCAMA)*, pages 256–265. SBC.

Tanoori, G., Soltani, A., and Modiri, A. (2024). Machine learning for urban heat island (uhi) analysis: Predicting land surface temperature (lst) in urban environments. *Urban Climate*, 55:101962.

Yin, H. and Zhao, X. (2024). Urban heat island analysis based on high resolution measurement data: A case study in beijing. *Sustainable Cities and Society*, 106:105389.